Talanta 114 (2013) 110–116

Contents lists available at ScienceDirect

Talanta

journal homepage: www.elsevier.com/locate/talanta

# Layer-by-layer self-assembly xylenol orange functionalized CdSe/CdS quantum dots as a turn-on fluorescence lead ion sensor

Qin Zhao [a,b], Xiaolong Rong [a], Li Chen [a], Hongbing Ma [c], Guanhong Tao [a,*]

[a] College of Chemistry, Chemical Engineering and Materials Science, Soochow University, Suzhou, Jiangsu 215123, China
[b] School of Chemistry and Chemical Engineering, Nantong University, Nantong, Jiangsu 226019, China
[c] Analytical and Testing Center, Soochow University, Suzhou, Jiangsu 215123, China

ARTICLE INFO

*Article history:*
Received 28 January 2013
Received in revised form
1 April 2013
Accepted 6 April 2013
Available online 12 April 2013

*Keywords:*
Quantum dots
Chitosan
Xylenol orange
Turn-on fluorescence sensor
Lead determination

ABSTRACT

A new turn-on fluorescence sensor based on xylenol orange (XO) functionalized CdSe/CdS quantum dots (QDs) is developed for the determination of lead ion. CdSe/CdS QDs were first modified by mercaptoacetic acid (MAA). The MAA-modified QDs were then capped with the natural biopolymer chitosan and the negatively charged XO. The XO-functionalized QDs were formed via the layer-by-layer self-assembly reaction. The fluorescence of the QDs was quenched by electron transfer mechanism after XO was bound to the QDs. Upon the addition of $Pb^{2+}$, a dramatic enhancement of the fluorescence intensity was observed, which resulted from the coordination between $Pb^{2+}$ and XO on QDs surface and the disruption of the electron transfer mechanism. Hence the fluorescence of the QDs was recovered. The recovery of the fluorescence intensity showed a good linear relationship with the concentration of $Pb^{2+}$ added from 0.05 to 6 μmol $L^{-1}$. A detection limit of 0.02 μmol $L^{-1}$ was achieved. This method was successfully applied to the determination of lead in real samples with satisfactory results.



## 1. Introduction

Lead, a toxic heavy metal, is widespread and persistent in the environment. Lead contamination is one of the most serious concerns to human health because even low-level lead exposure can cause a number of adverse health effects [1,2]. Therefore, monitoring of lead in the environment with high sensitivity is of great importance. Conventional analytical methods for lead detection, such as atomic absorption spectrometry [3,4], inductively coupled plasma mass spectrometry [5,6], and electrochemical methods [7,8], often require sophisticated equipment and trained personnel with high operational cost, making it difficult for real-time and on-site monitoring of lead. Thus, it is strongly demanded for the development of facile, rapid, inexpensive and highly sensitive methods for measurement of lead.

Quantum dots (QDs) possess attractive optical properties, including broad excitation and narrow emission spectra, size-tunable emission profiles, high photoluminescence (PL) quantum yields, and excellent photochemical stability [9–11]. These unique properties of QDs show considerable advantages over traditional organic fluorophores [12,13] in the applications of analytical chemistry, resulting in the increased use of QDs as fluorescence sensors [14–17]. A variety of QDs-based fluorescent sensors for the detection of heavy metals were developed with the advantages of high sensitivity, simplicity and low cost [18–21]. Chen and Rosenzweig [18] reported for the first time that $Cu^{2+}$ and $Zn^{2+}$ ions could be determined in aqueous medium by using CdS QDs capped with different ligands, such as thioglycerol and L-cysteine. Ying and his coworkers [19] developed a method for $Pb^{2+}$ detection using the glutathione-capped CdTe and ZnCdSe QDs. Han and his coworkers [20] described the detection of $Pb^{2+}$ based on the CdTe QDs capped with thioglycolic acid. Recent studies in our laboratory showed that diethyldithiocarbamate functionalized CdSe/CdS QDs could be used for the determination of $Cu^{2+}$ [21]. While many fluorescent sensors based on QDs have been successfully developed for heavy metals, there have been relatively few reports on $Pb^{2+}$ detection. And most of them generally displayed fluorescence quenching for $Pb^{2+}$ and awaited further improvements on linear range, sensitivity and selectivity.

In this study, we have investigated the use of layer-by-layer self-assembly technique to produce xylenol orange (XO) functionalized QDs for lead determination. By the layer-by-layer self-assembly technique, oppositely charged polyelectrolytes and active components are alternately self-assembled through the electrostatic adsorption on a host surface, such as charged flat substrates or nanoparticles, to fabricate ultrathin films and multilayer structures. The electrostatic self-assembly method has been proved to be a very simple approach for nanoparticles modification with favorable stability [22,23]. Chitosan, the natural biopolymer derived from alkaline deacetylation of chitin, is hydrophilic,

* Corresponding author. Tel.: +86 512 65226517; fax: +86 512 65223409.
*E-mail addresses:* taogh@suda.edu.cn, zqdaisy2009@163.com (G. Tao).

0039-9140/$ - see front matter © 2013 Elsevier B.V. All rights reserved.
http://dx.doi.org/10.1016/j.talanta.2013.04.016

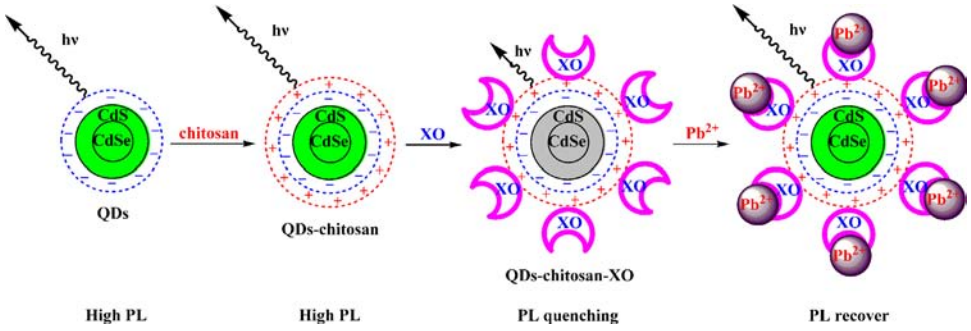


**Fig. 1.** Principle of XO-functionalized QDs synthesis and $Pb^{2+}$ detection.

nontoxic, biocompatible, and biodegradable. With the protonated amino groups in the repeating hexosaminide residue, chitosan stays positively-charged under weakly acidic conditions, which makes it possible to electrostatic self-assembly with anion [24]. XO, a negatively charged chromogenic reagent, has been classically used in spectrophotometric methods for the determination of lead. $Pb^{2+}$ can react with XO to form a stable complex of XO–Pb [25,26]. In this study, following the layer-by-layer self-assembly, CdSe/CdS QDs were functionalized by XO to prepare a turn-on fluorescence sensor for $Pb^{2+}$ detection. Our aim was to develop a sensitive and selective method for determination of $Pb^{2+}$ by combining the unique PL properties of QDs with the high affinity of XO to $Pb^{2+}$. The principle of XO-functionalized QDs synthesis and $Pb^{2+}$ detection is shown in Fig. 1. The synthesized lipophilic QDs were modified by mercaptoacetic acid (MAA) to achieve water solubility and lead to negative charge on QDs surface. The polycationic property of chitosan enabled electrostatic attachment of the polymer to the negatively charged QDs surface for achieving a positively charged surface distribution on the QDs. Then XO could easily self-assemble on the chitosan-capped QDs to form stable QDs-chitosan-XO conjugates by means of electrostatic interactions and the PL of the QDs was quenched by electron transfer mechanism. The PL of QDs was recovered with the addition of $Pb^{2+}$ because the electron transfer mechanism was disrupted when $Pb^{2+}$ was coordinated with the XO on QDs surface due to the high affinity of XO to $Pb^{2+}$. The developed QDs-based fluorescence sensor acts in a turn-on mode and offers a wide linear range for $Pb^{2+}$ measurement with high sensitivity and selectivity.

## 2. Experimental

### 2.1. Apparatus

The fluorescence spectra were recorded with an F-4600 fluorescence spectrophotometer (Hitachi, Japan). The X-ray photoelectron spectroscopy measurements were carried out in an AXIS Ultra$^{DLD}$ ultrahigh-vacuum surface analysis system (Kratos Analytical, UK). The UV absorption spectra were obtained on a U-2810 UV/vis spectrophotometer (Hitachi, Japan). An AA240FS atomic absorption spectrometer (Varian, USA) was used for the verification test. An Allegra 64R high-speed refrigerated centrifuge (Beckman, USA) was used to separate particles from solution. pH Values were measured by a Delta 320 pH meter (Mettler-Toledo, Switzerland).

### 2.2. Chemicals

Xylenol orange and other chemicals were purchased from Sinopharm Chemical Reagent Co., Ltd. (Shanghai, China). Standard stock lead solution was provided by National Analysis Center for Iron and Steel (Beijing, China). Certified reference material GBW(E)080398 (lead in simulated natural water) was obtained from National Research Center for Certified Reference Materials (Beijing, China). All chemicals used were of analytical-reagent grade except for nitric acid that was of guaranteed-reagent grade. The solutions were buffered with phosphate buffer solution (PBS), which was prepared by mixing appropriate amount of 1/15 mol $L^{-1}$ disodium hydrogen phosphate solution and 1/15 mol $L^{-1}$ potassium dihydrogen phosphate solution [27]. All solutions were prepared with ultrapure water, which was obtained from a Milli-Q system (Millipore, USA).

### 2.3. Synthesis of XO-functionalized QDs

The process of synthesis of XO-functionalized QDs involves two major steps. Firstly, the core–shell CdSe/CdS QDs modified by MAA were synthesized according to the reported method [28]. Secondly, the XO-functionalized QDs were prepared through a layer-by-layer self-assembly approach to conjugate the ligand XO on the surface of CdSe/CdS QDs. The procedure was briefly described below. Three milliliter of 1.2 μmol $L^{-1}$ CdSe/CdS QDs solution in pH 6.47 PBS was mixed with 3 mL of 0.01% w/v chitosan solution and shaking was used during 30 min. Then 3 mL of 50 μmol $L^{-1}$ XO solution was added to the above solution with shaking during 1 h, allowing XO to attach to the QDs through electrostatic interaction. The XO-functionalized QDs were separated from the excess of XO (non-attached) in the bulk solution by centrifugation and re-dispersion in 9 mL of pH 6.47 PBS for further use.

### 2.4. Procedure for spectrofluorometric detection of $Pb^{2+}$

One hundred microliter of standard or sample solution of lead and 300 μL of the prepared XO-functionalized QDs solution was added into 600 μL of pH 6.47 PBS and mixed thoroughly for 5 min. The solution was placed in a quartz cuvette with an optical path length of 10 mm. Then the fluorescence spectrum of the solution was recorded with the excitation wavelength of 380 nm. Both slit widths of excitation and emission were 10 nm. The fluorescence intensity of the solution at the maximum emission wavelength was used for quantitative analysis.

### 2.5. Sample preparation

Environmental samples were collected in the local industrial area. Water samples were filtered through mixed cellulose esters millipore membrane filter (0.45 μm pore size). Five milliliter of guaranteed-reagent grade nitric acid and 1 mL of hydrogen peroxide solution were then added into 100 mL filtered sample. The samples were heated and boiled for 30 min. Soil samples were prepared as described in Chinese Standard for the determination of lead in soil [29]. All samples were stored in opaque polyethylene bottles at 4 °C prior to analysis.

## 3. Results and discussion

### 3.1. Synthesis and characterization of XO-functionalized QDs

XO was bonded to the core/shell CdSe/CdS QDs based on the layer-by-layer self-assembly reaction to form XO-functionalized QDs. The CdSe/CdS QDs were first modified by MAA to achieve water solubility. The MAA on QDs was deprotonated, which led to negative charge on the surface of QDs [11]. Chitosan, which stayed positively-charged with protonated amino groups, was electrostatically attracted onto the negatively-charged MAA-modified QDs. Then QDs were capped with chitosan to achieve a positively-charged surface distribution and able to self-assemble with negatively-charged XO by means of electrostatic interaction to form the QDs-chitosan-XO conjugates. The as-prepared XO-functionalized QDs exhibited high optical stability without obvious decrease of fluorescence intensity over a period of two weeks.

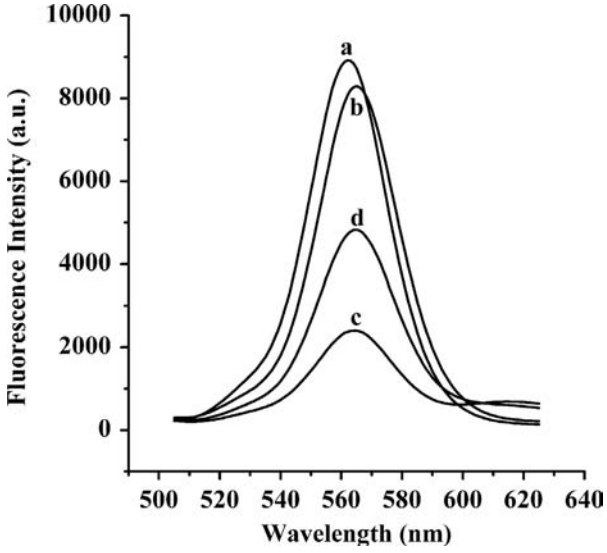


**Fig. 2.** Fluorescence spectra of QDs (a), QDs-chitosan (b), QDs-chitosan-XO (c) and QDs-chitosan-XO with 6 μmol $L^{-1}$ $Pb^{2+}$ (d).

Fluorescence spectra of MAA-modified CdSe/CdS QDs (QDs), chitosan-capped QDs (QDs-chitosan), XO-functionalized QDs (QDs-chitosan-XO) and XO-functionalized QDs with the addition of $Pb^{2+}$ were compared (Fig. 2). After the capping of chitosan, the QDs-chitosan retained the same sharp and narrow fluorescence emission of the QDs. The incorporation of the layer of chitosan caused negligible changes in the fluorescence intensity and a red-shift about 3 nm in the maximum emission, which suggested that no change occurred in the fluorescence properties of the QDs but increasing the particle size [30,31]. The fluorescence of the QDs-chitosan-XO conjugates was strongly quenched (circa 75%), which indicated that the assembly of XO on the surface of QDs was quite efficient. After the addition of $Pb^{2+}$, the fluorescence of XO-functionalized QDs was recovered, which enabled us to utilize XO-functionalized QDs as a sensitive fluorescent sensor for $Pb^{2+}$ detection. In contrast, the fluorescence of the "QDs-XO", which was prepared as described in the procedure for preparation of XO-functionalized QDs but without chitosan, had a negligible quenching and after the addition of $Pb^{2+}$, no enhancement of the fluorescence intensity was observed. This control experiment confirmed that the direct attachment of the negatively-charged XO on the negatively-charged MAA-modified CdSe/CdS QDs surface was not possible.

### 3.2. Optimization of XO concentration

Fig. 3(a) describes the fluorescence quenching behavior by the formation of XO-functionalized QDs. The fluorescence intensity decreases significantly with the increase of XO concentration. As shown in Fig. 3(b), there is a linear relationship between $I_0/I$ and XO concentration ($R=0.9988$), where $I_0$ and $I$ are the fluorescence intensity of the XO-functionalized QDs in the absence and presence of XO respectively, which is best described by a Stern–Volmer-type equation. As previously mentioned in other reported QDs-based methods [18,32], these indicate that XO has been bonded to the surface of the QDs through the formation of QDs-chitosan-XO conjugates.

The strongly quenched fluorescence of XO-functionalized QDs provided the basis of $Pb^{2+}$ detection, because the fluorescence could be recovered upon coordination of the XO on QDs surface

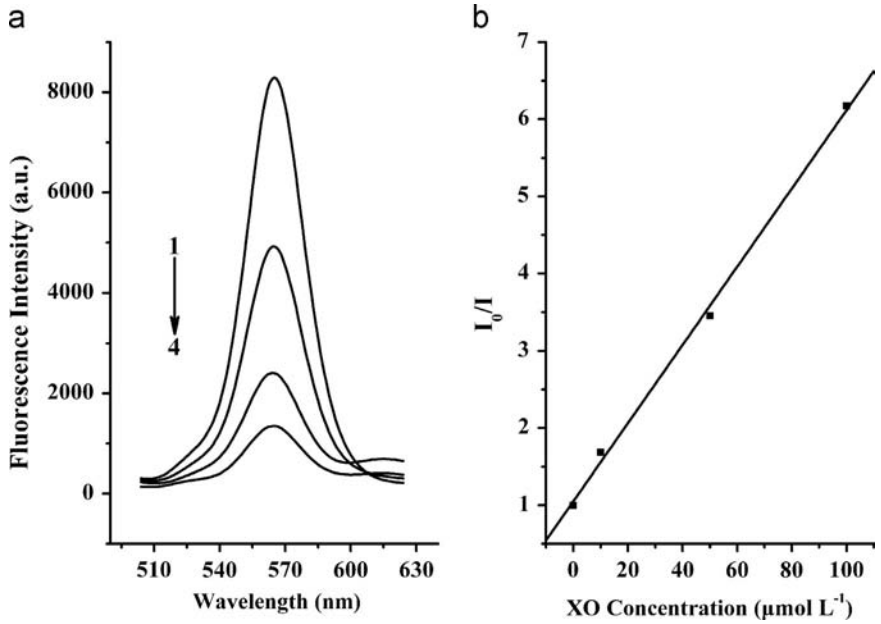


**Fig. 3.** (a) Fluorescence spectra of XO-functionalized QDs with the addition of different XO concentrations. The XO concentrations added for spectrum (1) to (4) were 0, 10, 50 and 100 μmol $L^{-1}$, respectively. (b) Stern–Volmer relationship between relative fluorescence intensity and XO concentration.

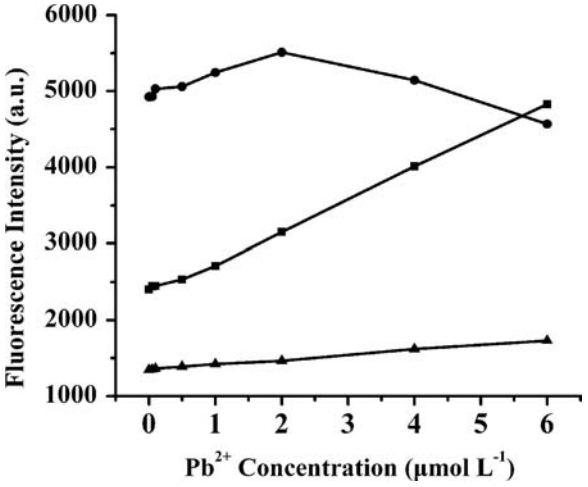


**Fig. 4.** Fluorescence response curves of XO-functionalized QDs with $Pb^{2+}$ at different concentrations of XO added: (●) 10 μmol $L^{-1}$ XO, (■) 50 μmol $L^{-1}$ XO and (▲) 100 μmol $L^{-1}$ XO.

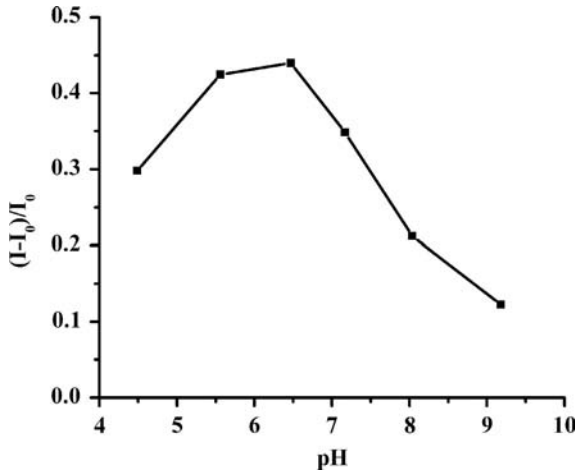


**Fig. 5.** Effect of pH on the extent of fluorescence enhancement of XO-functionalized QDs with the addition of 2 μmol $L^{-1}$ $Pb^{2+}$.

with $Pb^{2+}$. To optimize the XO concentration for preparation of XO-functionalized QDs, fluorescence response curves of XO-functionalized QDs with $Pb^{2+}$ at different concentrations of XO added were compared (Fig. 4). For $Pb^{2+}$ detection, attachment of XO at lower concentrations on the surface of the QDs introduced less ligands for $Pb^{2+}$ and caused lower quenching of the fluorescence of QDs, which led to a narrower linear range as shown in Fig. 4. On the other hand, higher XO concentrations on the surface of the QDs introduced more ligands for $Pb^{2+}$ and caused more quenching of the fluorescence of QDs, which led to the requirement of more $Pb^{2+}$ for the complexation with XO and affected the fluorescence response at low $Pb^{2+}$ concentrations. As a compromise between sensitivity and linear range, a solution of 50 μmol $L^{-1}$ XO was used here for the preparation of XO-functionalized QDs.

### 3.3. pH effect on fluorescence response

The effect of pH on fluorescence response of XO-functionalized QDs with $Pb^{2+}$ was investigated over the range of pH from 4.49 to 9.18 (Fig. 5). It can be seen that the enhancement of fluorescence intensity is pH-dependent. More enhancement of the fluorescence intensity occurred with the increase of pH from 4.49 to 6.47 and the enhancement achieved a maximum value at pH 6.47. At pH higher than 6.47, a decrease of the enhancement of fluorescence intensity was observed. The possible explanation may be that the MAA on the QDs is deprotonated at pH 6.47 and the amino groups of chitosan are protonated. At this pH the electrostatic interaction with the negatively-charged XO is quite strong to achieve the stable QDs-chitosan-XO conjugates and the efficient fluorescence response to $Pb^{2+}$. At lower pH the MAA on the QDs is protonated, which leads to a low negative charge on the QDs surface and produces a concomitant decrease in the attachment of subsequent layers of chitosan and XO. At higher pH the chitosan on the QDs is not fully protonated and its electrostatic interaction with negatively-charged XO is compromised, which leads to desorption of XO from the QDs surface. Both of them decrease the fluorescence response to $Pb^{2+}$. Considering the fluorescence response of XO-functionalized QDs with $Pb^{2+}$ to obtain maximum sensitivity, pH 6.47 was chosen for the determination of $Pb^{2+}$ studies.

### 3.4. Fluorescence response characteristics of XO-functionalized QDs for $Pb^{2+}$ detection

Upon the addition of $Pb^{2+}$, the fluorescence of XO-functionalized QDs was continuously recovered with the increase of $Pb^{2+}$ concentration and the extent of fluorescence enhancement was dependent on the concentration of $Pb^{2+}$ that could be used for the quantification of $Pb^{2+}$, as shown in Fig. 6. The calibration plot of $I/I_0$ versus $Pb^{2+}$ concentration showed a good linear relationship in the range of 0.05–6 μmol $L^{-1}$ ($R=0.9988$), where $I_0$ and $I$ are the fluorescence intensities of the XO-functionalized QDs in the absence and presence of $Pb^{2+}$ respectively. The detection limit was evaluated using $3\sigma/S$ and found to be 0.02 μmol $L^{-1}$, where $\sigma$ is the standard deviation of the blank signal and $S$ is the slope of the calibration plot. The U.S. Environmental Protection Agency (EPA) set the safety limit of lead in drinking water as 15 μg $L^{-1}$ or 75 nmol $L^{-1}$. As soon as the content of lead exceeds the standard, it can be detected out by our system. The relative standard deviation of 1.3% was obtained by 11 repeated detections of 2 μmol $L^{-1}$ $Pb^{2+}$. Without $Pb^{2+}$ the fluorescence intensity of XO-functionalized QDs stayed fairly stable and after addition of $Pb^{2+}$ the fluorescence intensity enhanced instantaneously and became stable within 5 min. Then the reaction time of 5 min was used in this study. It can be seen in Table 1 that the proposed fluorescence sensor exhibits excellent performances as compared to other already reported QDs-based methods for $Pb^{2+}$ determination. The previously reported methods have extensively used a fluorescence quenching mode. Various factors except for the analyte could induce the fluorescence quenching, which would affect the sensitive and selective detection of the analyte. Yet our sensor acts in a fluorescence enhancement mode, which can lessen the chance of false positives and offer high sensitivity and selectivity for $Pb^{2+}$ measurement. As can be seen in Table 1, the proposed method shows improved linear range, sensitivity and selectivity compared with other reported methods.

### 3.5. Mechanism to lead ion response

The fluorescence switch mechanism for the detection of $Pb^{2+}$ is schematically shown in Fig. 1. The positively-charged chitosan electrostatically capped onto the negatively-charged MAA-modified QDs, which caused negligible changes in the fluorescence intensity. Then negatively-charged XO was able to self-assemble on the chitosan-capped QDs through electrostatic interaction and quench fluorescence of the QDs by electron transfer mechanism. After the addition of $Pb^{2+}$ the coordination between $Pb^{2+}$ and XO on QDs surface disrupted the electron transfer mechanism and recovered the fluorescence of the QDs.

XO, the $Pb^{2+}$ receptor, is an efficient electron donor. In the XO-functionalized QDs, as proposed previously in other systems [33–35], the electron transferred from the XO to the valence band of the QDs following QDs photoexcitation, thereby preventing the radiative recombination process and quenching the fluorescence

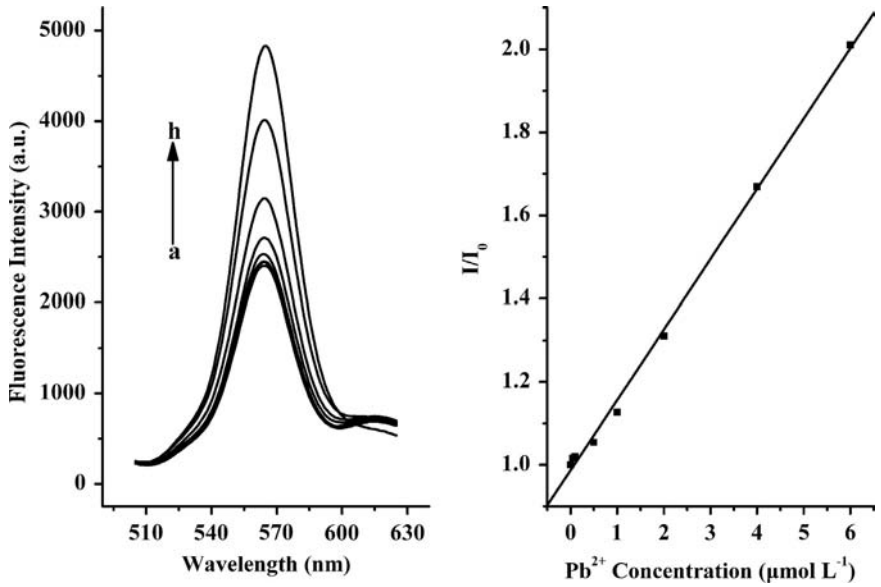


**Fig. 6.** Fluorescence spectra and calibration plot of XO-functionalized QDs after the addition of different $Pb^{2+}$ concentrations. The $Pb^{2+}$ concentrations for spectrum (a) to (h) were 0, 0.05, 0.1, 0.5, 1, 2, 4 and 6 μmol $L^{-1}$, respectively.

**Table 1**
Comparison of the QDs-based fluorescence sensors for $Pb^{2+}$ determination.

| QDs | Surface-modification | Measuring signal | Linear range | Detection limit | Interfering ion |
|---|---|---|---|---|---|
| ZnCdSe [19] | Glutathione | Fluorescence quenching | 0–200 nmol $L^{-1}$ | 20 nmol $L^{-1}$ | $Ag^{+}$, $Cu^{2+}$ |
| CdTe [20] | Thioglycolic acid | Fluorescence quenching | 2–100 μmol $L^{-1}$ | 0.27 μmol $L^{-1}$ | $Ag^{+}$, $Cu^{2+}$ |
| CdSe/CdS [This method] | Xylenol orange | Fluorescence enhancement | 0.05–6 μmol $L^{-1}$ | 0.02 μmol $L^{-1}$ | $Cu^{2+}$ |

of QDs. When $Pb^{2+}$ coordinated with the receptor XO on QDs surface, the electron donor got involved in the $Pb^{2+}$ coordination and the electron was lost on $Pb^{2+}$ complexation and was no longer available for the electron transfer mechanism, thereby reversing the XO quenching effect and restoring the fluorescence of QDs. Therefore, for the XO-functionalized QDs the fluorescence emission was "switched off" in the absence of $Pb^{2+}$ and "switched on" in the presence of $Pb^{2+}$.

X-ray photoelectron spectroscopy (XPS) was measured for the surface analysis of the synthesized nanoparticles, i.e., QDs, QDs-chitosan and QDs-chitosan-XO (Fig. 7). The functionalization of XO on QDs was demonstrated by XPS characterization. As could be seen in Fig. 7(a), the peak of N1s at 402 eV, which was attributed to nitrogen atoms in chitosan, appeared in the XPS spectra of QDs-chitosan. And the N1s peak at 402 eV was obviously enhanced in the XPS spectra of QDs-chitosan-XO, which was attributed to nitrogen atoms in XO. The appearance and enhancement of N1s peak provided the evidence of layer-by-layer self-assembly modification on QDs and confirmed that XO had been bound to the surface of QDs. To investigate the response mechanism of $Pb^{2+}$ on the XO-functionalized QDs, XPS spectra of QDs-chitosan-XO before and after the reaction with $Pb^{2+}$ were obtained, as shown in Fig. 7(b). After the reaction with $Pb^{2+}$, two new peaks of Pb4f appeared in the XPS spectra of QDs-chitosan-XO, indicating that the coordination between $Pb^{2+}$ and XO on QDs surface had occurred.

The possibility of fluorescence resonance energy transfer (FRET) which might cause fluorescence quenching by XO on QDs surface acting as acceptor was also examined. As shown in Fig. 8, the absorption spectrum of XO did not overlap the emission spectrum of the chitosan-capped QDs. The FRET mechanism was thus ruled out. Moreover, the fluorescence intensity of MAA-modified CdSe/CdS QDs and chitosan-capped QDs had no change after addition of $Pb^{2+}$. This control experiment revealed that $Pb^{2+}$ did not have any direct effect on the fluorescence of MAA-modified CdSe/CdS QDs and chitosan-capped QDs. It excluded the mechanism of the direct fluorescence enhancement of QDs by $Pb^{2+}$ or reaction between chitosan and $Pb^{2+}$. Therefore, it could be deduced that the electron transfer from XO to valence band of excited QDs originated prevention of radiative recombination (the electron transfer mechanism for the fluorescence quenching) and the coordination between $Pb^{2+}$ and XO on QDs surface originated disruption of the electron transfer mechanism and thus turn-on of the fluorescence was the primary mechanism for fluorescence switch of XO-functionalized QDs for the $Pb^{2+}$ detection in the present study.

### 3.6. Interference study

The influence of various coexistence ions on the fluorescence of XO-functionalized QDs in the determination of $Pb^{2+}$ (0.1 μmol $L^{-1}$) was tested to evaluate the selectivity of the proposed method. The results are shown in Table 2. It can be noted that the foreign ions investigated do not show any significant interference except $Cu^{2+}$. Only $Cu^{2+}$ at the concentration of 1 μmol $L^{-1}$ caused some interference with the detection of $Pb^{2+}$, showing the quenching of the fluorescence. This remains the limitation of our system despite its higher sensitivity and selectivity as compared to other lead ion detection systems based on QDs (Table 1). In the case of higher $Cu^{2+}$ concentration present in the sample, the interference might be eliminated with thiourea as a masking agent [36,37].

### 3.7. Application on environmental sample analysis

This method was successfully applied to the determination of lead in environmental samples and the results are presented in Table 3. The recoveries of the spiked samples and the relative

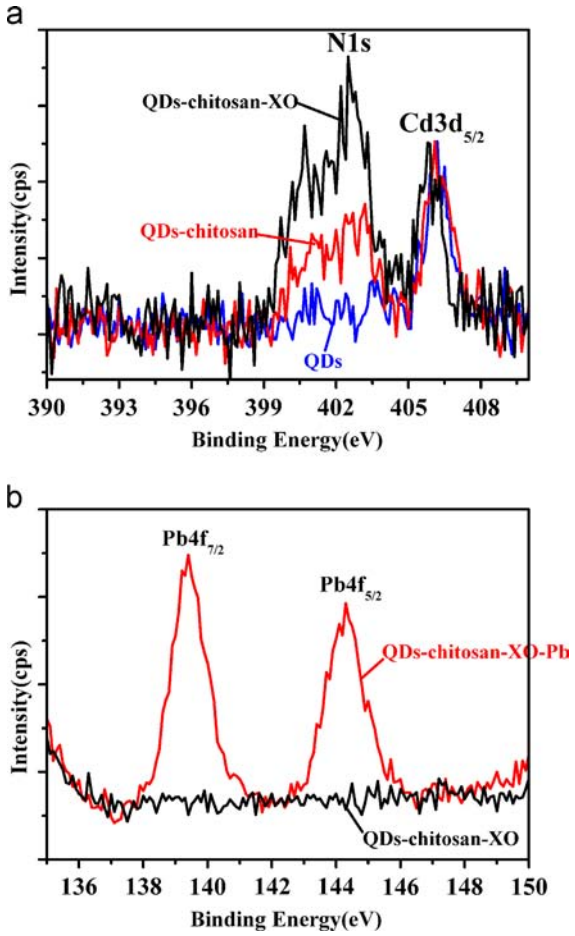


**Fig. 7.** (a) XPS spectra of N1s of QDs (blue), QDs-chitosan (red) and QDs-chitosan-XO (black). (b) XPS spectra of Pb4f of QDs-chitosan-XO before (black) and after (red) reaction with $Pb^{2+}$. (For interpretation of the references to color in this figure, the reader is referred to the web version of this article.)

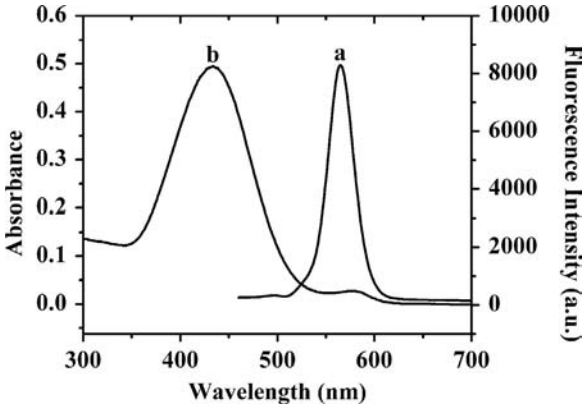


**Fig. 8.** The fluorescence spectrum of chitosan-capped QDs (a) and the UV–vis absorption spectrum of XO (b).

standard deviations ($n=3$) were generally satisfactory. The accuracy of the developed system was evaluated by analyzing the samples with graphite furnace atomic absorption spectrometry (GFAAS). The results obtained by the developed method were in fair agreement with the results given by the GFAAS method. In order to validate the procedure of the proposed method, a certified reference material GBW(E)080398 for lead was analyzed. The analytical result obtained was $0.49 \pm 0.02$ mg $L^{-1}$ ($n=3$), which was in good agreement with the certified value of $0.50 \pm 0.02$ mg $L^{-1}$.

**Table 2**
Interfering effect of foreign ions.[a]

| Foreign ion | Tolerance (μmol $L^{-1}$) | Relative error (%) |
|---|---|---|
| $Na^+$ | 100000 | −1.5 |
| $K^+$ | 100000 | −1.9 |
| $Mg^{2+}$ | 10000 | −0.3 |
| $Ca^{2+}$ | 1000 | −2.7 |
| $Al^{3+}$ | 100 | −1.4 |
| $Mn^{2+}$ | 100 | −0.6 |
| $Fe^{3+}$ | 100 | +3.4 |
| $Fe^{2+}$ | 100 | +2.6 |
| $Co^{2+}$ | 100 | −1.1 |
| $Ni^{2+}$ | 100 | −4.0 |
| $Zn^{2+}$ | 10 | −1.7 |
| $Cd^{2+}$ | 10 | +0.9 |
| $Ag^+$ | 10 | −3.0 |
| $Cu^{2+}$ | 1 | −6.1 |
| $Cl^-$ | 100000 | −1.5 |
| $NO_3^-$ | 10000 | +1.8 |
| $SO_4^{2-}$ | 1000 | −2.1 |
| $PO_4^{3-}$ | 1000 | −1.2 |

[a] The concentration of lead ion was 0.1 μmol $L^{-1}$.

**Table 3**
Determination of lead in environmental samples.

| Sample | Concentration[a] | | | Recovery (%) | RSD[c] (%) |
|---|---|---|---|---|---|
| | Added | Found by this method[b] | Found by GFAAS | | |
| Soil 1 | – | 57.14 | 59.77 | – | 1.4 |
| | 30 | 85.58 | 89.05 | 94.8 | 2.5 |
| Soil 2 | – | 34.39 | 35.97 | – | 1.7 |
| | 30 | 65.50 | 66.88 | 103.7 | 2.1 |
| River water | 15 | 14.42 | 15.96 | 96.1 | 3.3 |
| | 30 | 29.55 | 31.21 | 98.5 | 2.8 |
| Tap water | 15 | 14.73 | 16.08 | 98.2 | 2.4 |
| | 30 | 30.84 | 31.15 | 102.8 | 1.9 |

[a] The units of concentration are μg $g^{-1}$ for soil samples and μg $L^{-1}$ for aqueous samples.
[b] Mean of three measurements.
[c] Relative standard deviation ($n=3$).

## 4. Conclusions

In this paper, CdSe/CdS QDs were functionalized by XO based on a new strategy to develop a turn-on fluorescence sensor for $Pb^{2+}$ detection. Following a layer-by-layer self-assembly modification on the CdSe/CdS QDs, the QDs-chitosan-XO conjugates were prepared through electrostatic interaction. It exhibited excellent sensitivity and selectivity due to the specific and strong affinity of XO with $Pb^{2+}$ and the unique PL properties of QDs. The detection principle can be extended to the analysis of other ions if appropriate chelating reagents are bonded to QDs.

## Acknowledgments

The financial support of this study by the National Natural Science Foundation of China (Project nos. 20345006 and 20575043) is gratefully acknowledged.

## References

[1] H.L. Needleman, Human Lead Exposure, CRC Press, Boca Raton, FL, 1992.
[2] Centers for Disease Control and Prevention, Preventing Lead Poisoning in Young Children, CDC, Atlanta, 2005.

[3] D.I. Bannon, C. Murashchik, C.R. Zapf, M.R. Farfel, J.J. Chisolm Jr., Clin. Chem. 40 (1994) 1730–1734.
[4] J.E. Tahán, V.A. Granadillo, R.A. Romero, Anal. Chim. Acta 295 (1994) 187–197.
[5] S.K. Aggarwal, M. Kinter, D.A. Herold, Clin. Chem. 40 (1994) 1494–1502.
[6] H.W. Liu, S.J. Jiang, S.H. Liu, Spectrochim. Acta Part B 54 (1999) 1367–1375.
[7] T. Sokalski, A. Ceresa, T. Zwickl, E. Pretsch, J. Am. Chem. Soc. 119 (1997) 11347–11348.
[8] K. Crowley, J. Cassidy, Electroanalysis 14 (2002) 1077–1082.
[9] H. Weller, Angew. Chem. Int. Ed. 32 (1993) 41–53.
[10] M. Bruchez Jr., M. Moronne, P. Gin, S. Weiss, A.P. Alivisatos, Science 281 (1998) 2013–2016.
[11] W.C.W. Chan, S. Nie, Science 281 (1998) 2016–2018.
[12] C.T. Chen, W.P. Huang, J. Am. Chem. Soc. 124 (2002) 6246–6247.
[13] J.Y. Kwon, Y.J. Jang, Y.J. Lee, K.M. Kim, M.S. Seo, W. Nam, J. Yoon, J. Am. Chem. Soc. 127 (2005) 10107–10111.
[14] W.J. Jin, J.M. Costa-Fernández, R. Pereiro, A. Sanz-Medel, Anal. Chim. Acta 522 (2004) 1–8.
[15] J. Liang, S. Huang, D. Zeng, Z. He, X. Ji, X. Ai, H. Yang, Talanta 69 (2006) 126–130.
[16] R. Kuang, X. Kuang, S. Pan, X. Zheng, J. Duan, Y. Duan, Microchim. Acta 169 (2010) 109–115.
[17] X. Zhou, Y. Meng, H. Ma, G. Tao, Microchim. Acta 173 (2011) 259–266.
[18] Y. Chen, Z. Rosenzweig, Anal. Chem. 74 (2002) 5132–5138.
[19] E.M. Ali, Y. Zheng, H. Yu, J.Y. Ying, Anal. Chem. 79 (2007) 9452–9458.
[20] H. Wu, J. Liang, H. Han, Microchim. Acta 161 (2008) 81–86.
[21] J. Wang, X. Zhou, H. Ma, G. Tao, Spectrochim. Acta Part A 81 (2011) 178–183.
[22] S. Jaffar, K.T. Nam, A. Khademhosseini, J. Xing, R.S. Langer, A.M. Belcher, Nano Lett. 4 (2004) 1421–1425.
[23] M.J. Ruedas-Rama, E.A.H. Hall, Analyst 134 (2009) 159–169.
[24] M.N.V. Ravi Kumar, React. Funct. Polym. 46 (2000) 1–27.
[25] J. Körbl, R. Přibil, A. Emr, Collect. Czech. Chem. Commun. 22 (1957) 961–966.
[26] B. Řehák, J. Körbl, Collect. Czech. Chem. Commun. 25 (1960) 797–802.
[27] Handbook of Analytical Chemistry, vol. 1, Chemical Industry Press, Beijing, 1997.
[28] Q. Zhao, X. Rong, H. Ma, G. Tao, J. Hazard. Mater. 250–251 (2013) 45–52.
[29] National Environmental Protection Agency, GB/T 17141-1997, Soil Quality-Determination of Lead, Cadmium–Graphite Furnace Atomic Absorption Spectrophotometry, NEPA, Beijing, 1997.
[30] M. Gao, S. Kirstein, H. Möhwald, A.L. Rogach, A. Kornowski, A. Eychmüller, H. Weller, J. Phys. Chem. B 102 (1998) 8360–8363.
[31] W.B. Tan, N. Huang, Y. Zhang, J. Colloid Interface Sci. 310 (2007) 464–470.
[32] C. Bo, Z. Ping, Anal. Bioanal. Chem. 381 (2005) 986–992.
[33] A.P. de Silva, H.Q.N. Gunaratne, T. Gunnlaugsson, A.J.M. Huxley, C.P. McCoy, J.T. Rademacher, T.E. Rice, Chem. Rev. 97 (1997) 1515–1566.
[34] I.S. Liu, H.H. Lo, C.T. Chien, Y.Y. Lin, C.W. Chen, Y.F. Chen, W.F. Su, S.C. Liou, J. Mater. Chem. 18 (2008) 675–682.
[35] J.F. Callan, R.C. Mulrooney, S. Kamila, B. McCaughan, J. Fluoresc. 18 (2008) 527–532.
[36] Q.G. Liao, Y.F. Li, C.Z. Huang, Talanta 71 (2007) 567–572.
[37] A.N. Liang, L. Wang, H.Q. Chen, B.B. Qian, B. Ling, J. Fu, Talanta 81 (2010) 438–443.